

The Scaling of the RMS with Dwell Time in NANOGrav Pulsars

Emma Handzo¹, B. Christy, Andrea N. Lommen, Delphine Perrodin²

*Department of Physics and Astronomy, Franklin and Marshall College
415 Harrisburg Pike, Lancaster, Pennsylvania, 17603*

ABSTRACT

Pulsar Timing Arrays (PTAs) are collections of well-timed millisecond pulsars that are being used as detectors of gravitational waves (GWs). Given current sensitivity, projected improvements in PTAs and the predicted strength of the GW signals, the detection of GWs with PTAs could occur within the next decade. One way we can improve a PTA is to reduce the measurement noise present in the pulsar timing residuals. If the pulsars included in the array display uncorrelated noise, the root mean square (RMS) of the timing residuals is predicted to scale as $T^{-1/2}$, where T is the dwell time per observation. In this case, the sensitivity of the array can be increased by increasing T . We studied the 17 pulsars in the five year North American Nanohertz Observatory for Gravitational Waves (NANOGrav) data set to determine if the noise in the timing residuals of the pulsars observed was consistent with this property. For comparison, we performed the same analysis on PSR B1937+21, a pulsar that is known to display red noise. With this method, we find that 15 of the 17 NANOGrav pulsars have timing residuals consistent with the inverse square law. The data also suggest that these 15 pulsars can be observed for up to eight times as long while still exhibiting an RMS that scales as root T .

1. Introduction

A Pulsar Timing Array (PTA) is a collection of millisecond pulsars monitored frequently for imprints of gravitational waves (GWs). Currently there are three PTA collaborations: the European Pulsar Timing Array (EPTA) (Ferdman et al. 2010), the Parkes Pulsar Timing Array (PPTA) (Manchester et al. 2013), and the North American Nanohertz Observatory for Gravitational Waves (NANOGrav) (Jenet et al. 2009). In partnership with each other, they make up the International Pulsar Timing Array (IPTA) (Hobbs et al. 2010). Using a PTA as an instrument for GW detection, these collaborations search for correlated disturbances in the pulse arrival times.

Siemens et al. (2013) estimate that detection of GWs will happen in the next decade, with uncertainties arising from unknowns such as the amplitude of the GW signal, the number of pulsars

¹now at the University of Texas Rio Grande Valley

²now at INAF - Osservatorio Astronomico di Cagliari, Cagliari, Italy

added to the array in the future, and the noise level of the pulsar themselves. The appraisal of pulsar noise is key in estimating the sensitivity of the experiment, and in this manuscript we employ a simple test to provide some knowledge of the noise behavior in the NANOGrav pulsars. We are concerned specifically with the root mean square (RMS) residual as an estimator for the noise amplitude. We summarize briefly here the expected scaling of the sensitivity of the overall experiment with RMS. Siemens et al. (2013) calculates the average GW signal-to-noise (GW S/N) ratio for a PTA that samples the pulsars at regular intervals, assuming each of these pulsars has the same uncorrelated noise level. They show that in the weak-signal limit (where the uncorrelated noise dominates the GW signal), the GW S/N is inversely proportional to the square of the RMS. In the intermediate regime (where the uncorrelated noise is roughly equivalent with the GW signal), the GW S/N has a more complicated relationship to the RMS, but the sensitivity to GWs still increases with decreasing RMS. Finally, in the strong-signal limit (where the GW signal dominates the noise), the GW S/N is determined by the cadence of the observations. Reducing the RMS residual is therefore a crucial PTA strategy until we find ourselves in the strong-signal regime.

Although there are multiple avenues for noise (and therefore RMS) reduction, this paper focuses on the possibility of decreasing the RMS by increasing the *dwell* time, the amount of observation time spent on a pulsar to obtain a single arrival time. We roughly expect a pulsar’s timing residuals to be Gaussian distributed and, consequently, we expect the RMS of the residuals to scale as the inverse square root of the dwell time. Thus we commonly assume that we can improve the sensitivity of the experiment simply by increasing the dwell time (Jenet et al. 2005, 2006).

The presence of red noise changes the situation. There are many possible sources of the red noise: measurement noise, GWs (Lommen & Backer 2001), intrinsic noise (Hobbs, Lyne, & Kramer 2006), objects orbiting the pulsar (Hobbs, Lyne, & Kramer 2006; Shannon et al. 2013), or interstellar medium (ISM) effects (Hemberger & Stinebring 2008). Red noise likely exists at some level in all pulsars, and it becomes more important as we reduce the white noise. When red noise begins to dominate the overall noise, we can no longer expect the RMS to decrease with increasing dwell time (Jenet et al. 2006).

The goal of this paper is to determine the extent to which increasing the dwell time on NANOGrav pulsars will reduce the noise in the timing residuals. To test our ability to decrease the RMS, we cannot go back and increase the amount of dwell time for each pulsar in past observations, but we can mimic this by adding up adjacent observations to simulate longer dwell times. Throughout the paper, we use “N”, the number of adjacent observations being added together, which is a surrogate to “T”, the dwell time. This allows us to discuss the “root N” behavior of the pulsars, which should be read analogous to “root T”. This is a common test done in pulsar timing (Helfand, Manchester, & Taylor 1975; Cordes & Greenstein 1981; Liu et al. 2012; Dolch et al. 2014). This paper is organized as follows: in §2, we demonstrate the expectation of the root N dependence of the RMS residual, highlighting the conditions that must be met. In §3, we describe how we applied this to the NANOGrav data and present the results. In §4, we discuss whether the pulsars display this dependence and the limits to the test resulting from the timing model fit. In

§5, we summarize our findings, discuss our results in the context of EPTA and PPTA data, and suggest how future work will help us understand the situation better..

2. The $N^{-1/2}$ Test

A timing model for a pulsar is generated after a pulsar has been observed for a long period of time. It predicts when the next pulse from the pulsar should arrive (Hobbs, Lyne, & Kramer 2006). The timing model yields a timing residual, which is the measured pulse arrival time minus the predicted pulse arrival time:

$$t = t_{\text{measured}} - t_{\text{predicted}} \quad (1)$$

We typically use the RMS of these residuals as a measure to characterize the total noise in the dataset. A lower RMS residual is indicative of residuals that are close to zero. While many pulsars follow the trend $\text{RMS} \propto N^{-1/2}$, where N is the number of observations made, not all pulsars do. We need to determine which pulsars' RMS residual decreases with increasing N and which do not, so we can make informed choices about which pulsars should be included in the PTA and for how long they should be observed.

We want to determine the effect of increasing the dwell time on the RMS of a pulsar. As a proxy, we make this comparison by averaging N successive points together. Then, we study how the RMS of the timing residuals changes as a function of N .

First, let us demonstrate the existence of the root N relation and the conditions under which we expect it to hold true. We average an original data set \mathbf{T} by every N points. This gives us a new data set, $\mathbf{T}' = \{t'_1, t'_2 \dots t'_M\}$, where M is the number of points in the new, averaged dataset. If Q is the total number of points in the original dataset, then $Q=M \times N$. To create \mathbf{T}' we first create sets of samples of \mathbf{T} of every N th number: $\mathbf{T}_1 = \{t_1, t_{N+1}, \dots\}$, $\mathbf{T}_2 = \{t_2, t_{N+2}, \dots\}$ and so on. The new points are calculated using $\mathbf{T}' = \{\frac{t_1+t_2+\dots+t_N}{N}, \frac{t_{N+1}+t_{N+2}+\dots+t_{2N}}{N}, \dots\} = \frac{\mathbf{T}_1+\mathbf{T}_2+\dots+\mathbf{T}_N}{N}$. The relationship between $\text{Var}(\mathbf{T}')$ and $\text{Var}(\mathbf{T})$, becomes:

$$\text{Var}(\mathbf{T}') = \frac{\text{Var}(\mathbf{T})}{N} \quad (2)$$

It follows trivially that:

$$\text{RMS}_{\mathbf{T}'} = \frac{1}{\sqrt{N}} \text{RMS}_{\mathbf{T}} \quad (3)$$

It is the relationship contained in Equation 3 that we investigate in this paper. This relationship has been studied by many other authors (such as Helfand, Manchester, & Taylor (1975); Cordes & Greenstein (1981); Jenet et al. (2005); Liu et al. (2012)), whose results were similar to ours. Note that the veracity of the relation depends upon the residuals being statistically independent. If this is not the case, e.g. in red noise, $\text{Var}(P_1 + P_2) \neq \text{Var}(P_1) + \text{Var}(P_2)$, and Equation 2 is not valid. Also, if the distribution is non-stationary, i.e. it is changing in time, then the relationship

$\text{Var}(P_1) \neq \text{Var}(P_2)$ would be true, and we would not expect the RMS of the pulsars to decline as $N^{-1/2}$. Recent works by Ellis, Jenet, & McLaughlin (2012) and references therein state that the NANOGrav data appears to display noise patterns that allow us to assume stationary statistics with this data set.

In PTA data sets, each data point is assigned an uncertainty, σ , based on the S/N of the data taken. The uncertainty can vary due to a variety of conditions, such as scintillation from the ISM. To account for this variation, our averaging was performed by weighting the points with $1/\sigma^2$. We performed a simulated test to verify if residuals with unequal errors still follow the root N trend. We took the J1713+0747 dataset and replaced the data points with values drawn from a Gaussian distribution. The unequal uncertainties from the original dataset were kept. We performed the test on this dataset and found that the RMS of the simulated data follows the expected root N relationship even with the unequal errors.

3. Analysis

In this paper, we analyze the residuals of the timing data set on the 17 pulsars presented by Demorest et al. (2013) in order to determine whether the NANOGrav pulsars’ timing noise follows the root N relationship. Currently the NANOGrav pulsars are allotted roughly equal observing time of 15-45 minutes within NANOGrav’s total telescope time. The 17 pulsars that were examined in this paper were observed from 2005 to 2010 at either the Arecibo Observatory or the Green Bank Telescope, in frequencies ranging from 330MHz to 2500MHz. The one exception is PSR J1713+0747, which was observed at both telescopes.

We demonstrated in the previous section that we expect the RMS residual to be proportional to $N^{-1/2}$ for pulsars whose residuals display uncorrelated noise when calculating the RMS of a residual data set $\mathbf{T} = t_1, t_2, \dots, t_Q$. For our data set, N is the number of data points that are being averaged together. Since each data point is roughly the same observation time, N is directly proportional to the total dwell time, e.g. if you average every two points together, the resulting point is the expected timing residual of that pulsar being observed for twice as long. As discussed in §2, these data have unequal uncertainties so we weight them by $1/\sigma^2$ to account for the fact that some observations are not as accurate as others, due to the observing conditions.

In the NANOGrav observing program that Demorest et al. (2013) uses, data from an observing epoch are split into 4MHz sub-bands in order to study the frequency evolution of the profile in greater detail. As we are interested in the behavior over long time scales (Wackerly, Mendenhall III, & Scheaffer

2008), we begin by averaging over these frequency sub-bands as follows:

$$t_i = \frac{\sum_{j=1}^{M_i} (t_{i,j} / \sigma_{i,j}^2)}{\sum_{j=1}^{M_i} (1 / \sigma_{i,j}^2)} \quad (4)$$

where $t_{i,j}$ is the j th residual on day i , with $\sigma_{i,j}$ representing the TOA error, resulting from the cross-correlation with a template (see Demorest et al. (2013)), and M_i is the total number of residual points on this day. Uncertainties are given by the standard deviation:

$$\sigma_i = \sqrt{\frac{\sum_{j=1}^{M_i} ((t_{i,j} - \bar{t})^2 / \sigma_{i,j}^2)}{(M_i - 1) \sum_{j=1}^{M_i} (1 / \sigma_{i,j}^2)}} \quad (5)$$

where \bar{t} is the weighted mean of each data set (Wackerly, Mendenhall III, & Scheaffer 2008). With the large number of points in a given epoch, typically ~ 15 , we expect the fit to the average to follow a χ^2 distribution with $M - 1$ degrees of freedom, and we weight the uncertainties by the reduced χ^2 . These calculations yield a reduced new data set, (\mathbf{T}) that depicts one timing residual (t_i) and the standard deviation of the timing residual (σ_i) for each observing day i . We use these reduced data sets to inspect how the RMS residual changes if we observe each pulsar for longer periods of time, or in other words, as we increase N .

To begin, we calculate the weighted RMS (WRMS) of the epoch-averaged residuals, $\mathbf{T} = \{t_1, t_2, \dots, t_Q\}$:

$$\text{WRMS} = \sqrt{\frac{\sum_{i=1}^Q ((t_i - \bar{t})^2 / (\sigma_i)^2)}{\sum_{i=1}^Q (1 / (\sigma_i)^2)}}. \quad (6)$$

The uncertainty in this residual WRMS is given by:

$$\sigma_{\text{WRMS}} = \sqrt{\frac{1}{\sum_{i=1}^Q (1 / (\sigma_i)^2)}} \quad (7)$$

Next, we average every N residual data points that are consecutive in time to make a new data set \mathbf{T}' just as described above in Equation 4. The error for these points is found using error propagation

and is similar to Equation 5. Note that, unlike when we calculated the daily averaging, we do not weight the uncertainty by χ^2 since the number of points is small and the χ^2 distribution is not well behaved. We let N have the range $\{1, B\}$ where B is equal to the number of residuals in the original set divided by the number of points being averaged together. Again, the residual WRMS and σ_{WRMS} are calculated using Equations 6 and 7.

We examine the rate at which the WRMS of the timing residuals for each of the NANOGrav pulsars decline with respect to N . The majority of the NANOGrav pulsars were observed in both a low-frequency (generally 800 MHz) and a high-frequency (generally 1400 MHz) band. The exceptions to this are PSR J1713+0747, which was observed in the high and low bands at both the Arecibo Observatory (AO) and the Green Bank Telescope (GBT), and PSRs B1953+29, J1853+1308 and J1910+1256, which were originally part of another project so we have only the 1410 MHz observations for most of the observation time (Demorest et al. 2013; Gonzalez et al. 2011).

To quantify the extent each pulsar follows the root N behavior, we find the least squares fit of the data to $\text{WRMS} = aN^{-1/2}$, where a is the only fitted parameter. For each fit, a reduced χ^2 was found using:

$$\text{Reduced } \chi^2 = \frac{\sum_i ((\text{WRMS}_i - \text{fit})^2 / \sigma_i^2)}{K_{\text{dof}}} \quad (8)$$

where K_{dof} is the number of degrees of freedom found with $K_{\text{dof}} = K_{\text{points}} - K_{\text{parameters}} - 1 = K_{\text{points}} - 2$.

Figures 1, and 2 are consistent with a WRMS proportional to $N^{-1/2}$ for PSRs J0030+0451, J0613–0200, J1012+5307, J1455–3330, J1600–3053, J1744–1134, B1855+09, J1909–3744, J1918–0642, J2145–0750 and J2317+1439. The reduced χ^2 values of the fit for each of the pulsars are presented in Table 1. The pulsars just mentioned have reduced χ^2 values close to 1 in the high frequencies, but the low frequencies give very small values. As described in Demorest et al. (2013), the low frequency band WRMS is expected to be suppressed because of the dispersion measure (DM) fitting, leading to small reduced χ^2 values, see §4. The best fit $\text{WRMS} = aN^{-1/2}$ line is shown in each Figures 1-9.

χ^2 values

Table 1:: Table 1 shows the goodness of the fit between the expected RMS value fitted to a slope of $N^{-1/2}$. The goodness of the data is measured by the χ^2 and reduced χ^2 .

Pulsar	Frequency (MHz)	Observatory	χ^2	Reduced χ^2
J0030+0451	1410	AO	4.46914295786	0.558642869733
J0613-0200	1390	GBT	12.0463663442	0.708609784953
J1012+5307	1390	GBT	14.2027958984	0.835458582261
J1455-3330	1390	GBT	14.0405246474	0.825913214552
J1600-3053	1400	GBT	2.11653100526	0.211653100526
J1640+2224	1400	AO	84.0567098794	8.40567098794
J1643-1224	1390	GBT	80.2630069467	4.72135334981
J1713+0747	1400	GBT	4.54006173273	0.267062454867
J1713+0747	2500	AO	10.9673468661	0.913945572174
J1744-1134	1380	GBT	28.6140639164	1.68318023038
J1853+1308	1410	AO	8.23077276824	0.54871818455
B1855+09	1410	AO	13.7537378327	1.05797983329
J1909-3744	1400	GBT	19.2218747739	1.37299105528
J1910+1256	1410	AO	40.98978419	3.15306032231
J1918-0642	1400	GBT	16.0827033438	0.946041373163
B1937+21	1405	AO	271657.658795	15979.8622821
B1953+29	1410	AO	10.0596679919	1.11774088799
J2145-0750	1400	GBT	10.267139863	1.14079331812
J2317+1439	430	AO	9.20820969886	0.708323822989

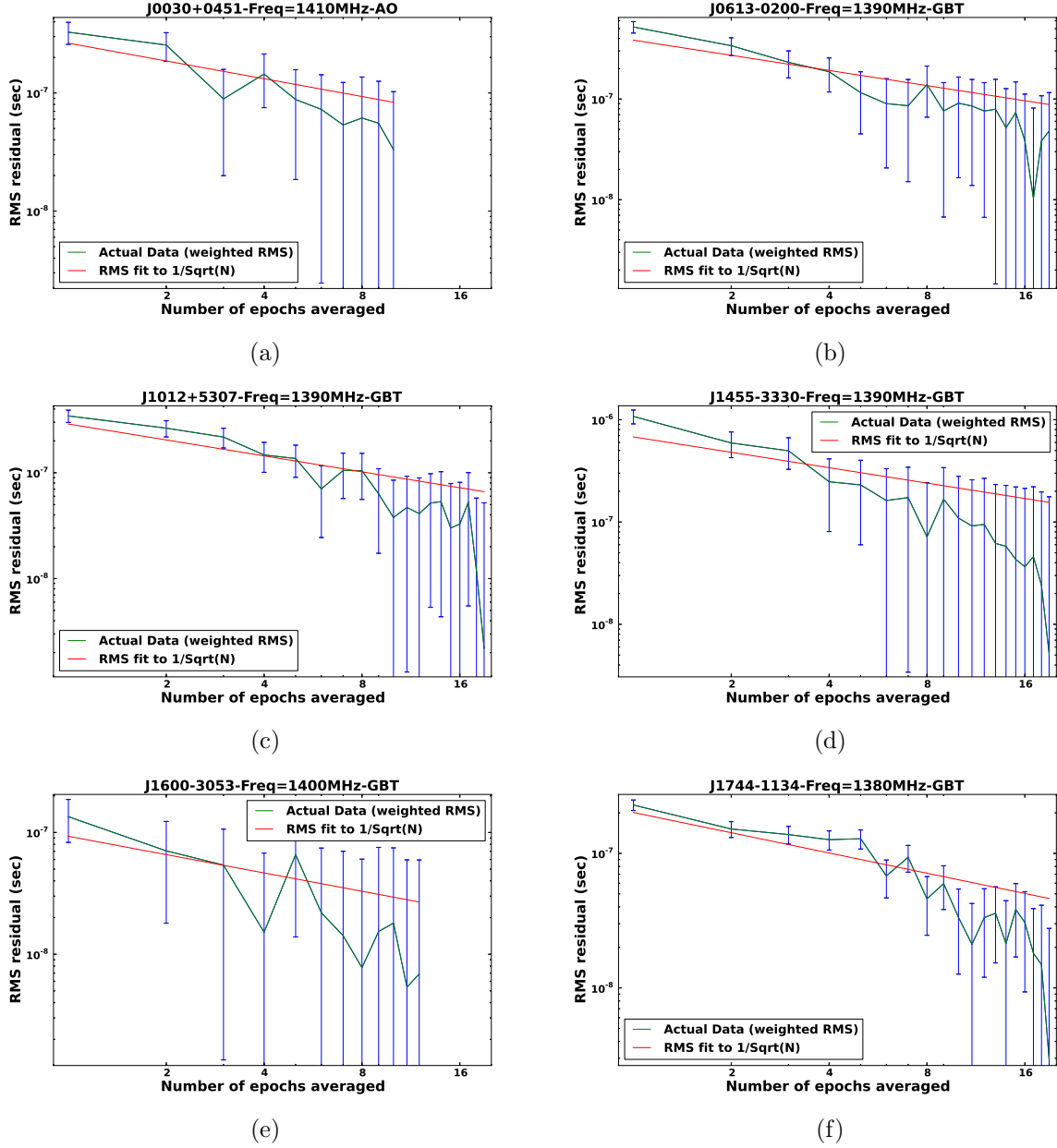


Fig. 1.—: RMS residual vs. the number of residuals averaged for the PSR J0030+0451 when observed at 1410 MHz (Panel a), PSR J0613–0200 at 1410 MHz (Panel b), PSR J1012+5307 at 1390 MHz (Panel c), PSR J1455–3330 at 1390 MHz (Panel d), PSR J1600–3053 at 1400 MHz (Panel e), and PSR J1744–1134 at 1380 MHz (Panel f). The solid line represents the RMS fit to $N^{-1/2}$. The plots show that within uncertainties, the RMS residual is proportional to $N^{-1/2}$ for these pulsars.

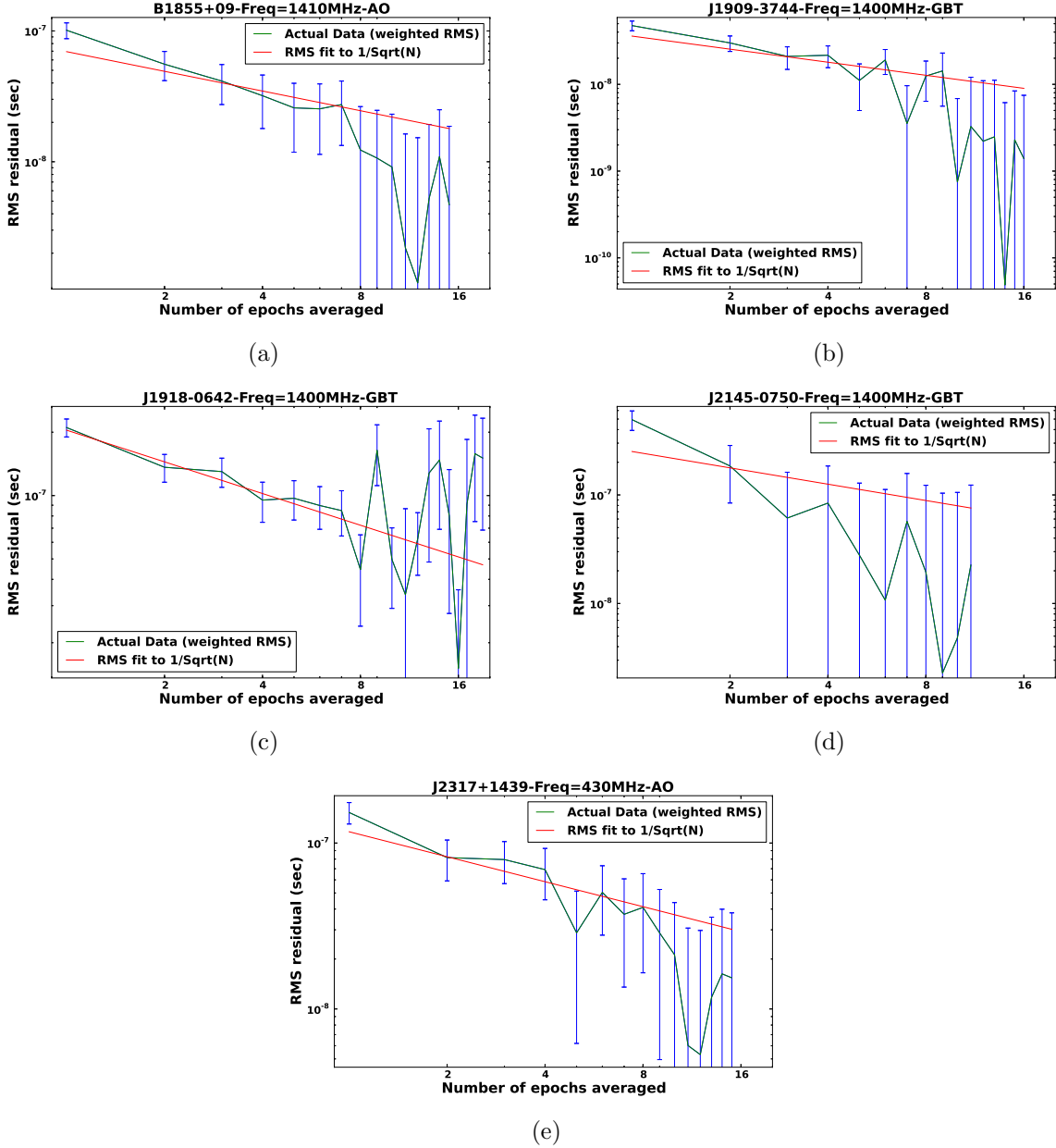


Fig. 2.—: RMS residual vs. the number of residuals averaged for the B1855+09 when observed at 1410 MHz (Panel a), PSR J1909–3744 at 1400 MHz (Panel b), PSR J1918–0642 at 1400 MHz (Panel c), PSR J2145–0750 at 1400 MHz (Panel d) and PSR J2317+1439 at 430 MHz (Panel e). The solid line represents the RMS fit to $N^{-1/2}$. The plots show that within uncertainties, the RMS residual is proportional to $N^{-1/2}$ for these pulsars.

For PSRs B1953+29, J1853+1308 and J1910+1256 (Figure 3), we only have one frequency band as mentioned previously. This limits the ability to correct for DM. Despite this, the RMS

still shows a general decreasing trend.

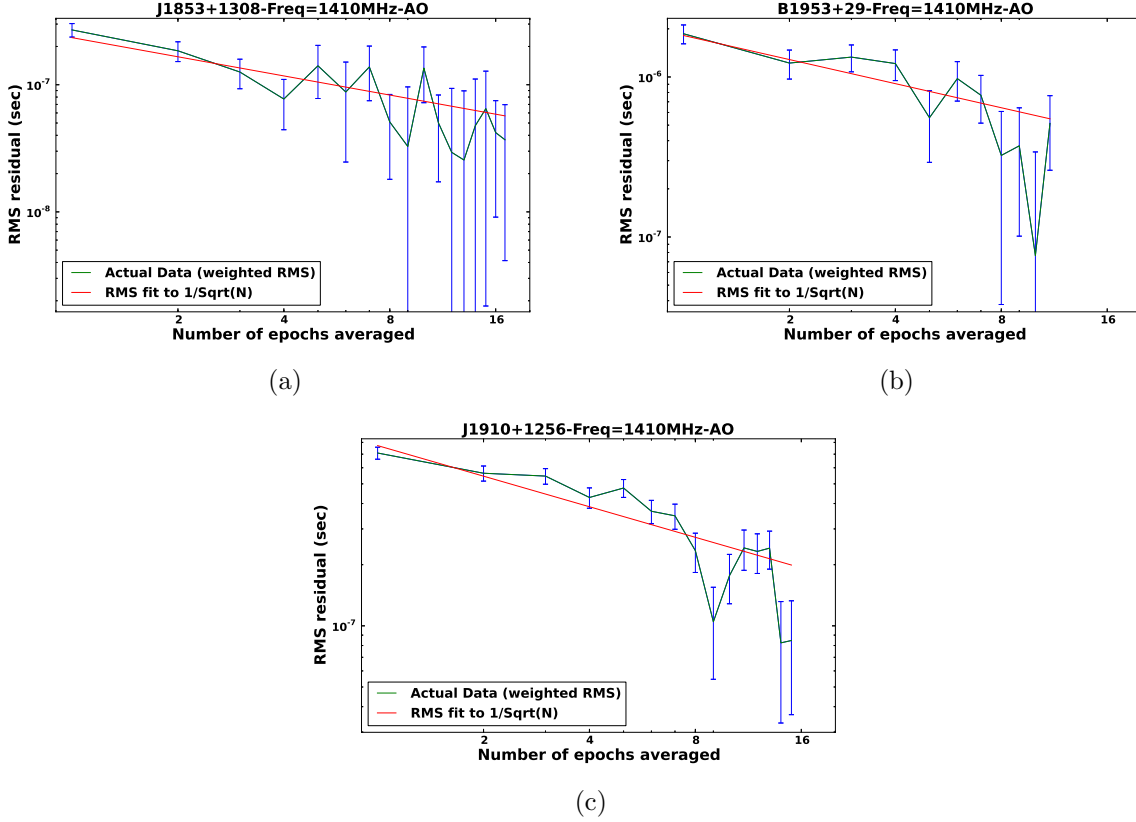


Fig. 3.—: RMS residual vs. the number of residuals averaged for PSR J1853+1308 when observed at 1410 MHz (Panel a), and PSR B1953+29 at 1410 MHz (Panel b) and PSR J1910+1256 at 1410 MHz (Panel c). The solid line represents the RMS fit to $N^{-1/2}$. The plots show that within uncertainties, the RMS residual is proportional to $N^{-1/2}$ for these pulsars.

There were only two pulsars that had a large reduced χ^2 , which is also evident when examining the plots in Figure 4. These were also pulsars identified by both Demorest et al. (2013) and Perrodin et al. (2015) as showing the largest evidence for red noise in the NANOGrav dataset.

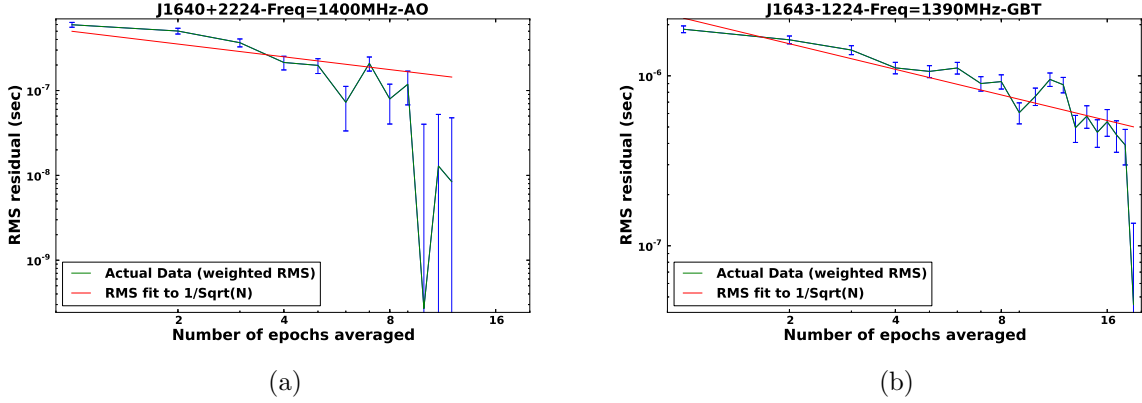


Fig. 4.—: RMS residual vs. the number of residuals averaged for the PSR J1640+2224 when observed at 430 MHz (Panel a) and 1400 MHz (Panel b), and PSR J1643–1224 at 830 MHz (Panel c) and 1390 MHz (Panel d). The solid line represents the RMS fit to $N^{-1/2}$. The plots show that within uncertainties, the RMS residual is proportional to $N^{-1/2}$ for these pulsars.

PSR 1713+0747 (Figure 5) is unique in that it was observed at two different observatories. While each of the plots vary in shape, when looking at the overall trends displayed, the RMS residual decreases at the expected rate of $N^{-1/2}$.

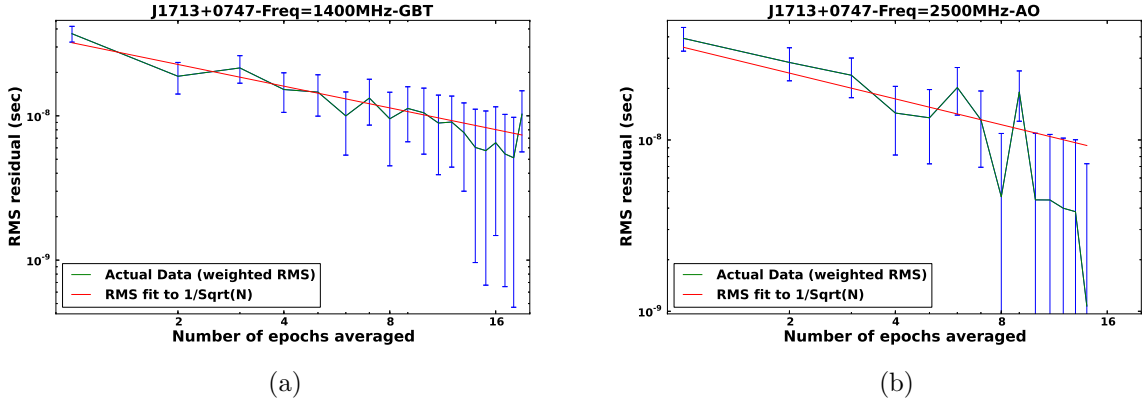


Fig. 5.—: RMS residual vs. the number of residuals averaged for the pulsar when observed at 840 MHz (Panel a), at 1400 Mhz (Panel b), 1410 MHz (Panel c) and 2500 MHz (Panel d). The solid line represents the RMS fit to $N^{-1/2}$. All plots show that within uncertainties, the RMS residual of PSR J1713+0747 follows the expected rate of decline of $N^{-1/2}$.

For comparison, we analyzed data for PSR B1937+21 (Figure 6) from Lommen (2001) in the same way. As a millisecond pulsar with a strong red noise signal, this provides an important test to ensure our method will demonstrate a noise floor in the presence of strong red noise. We found the RMS does not decrease at all for this pulsar as more points are averaged.

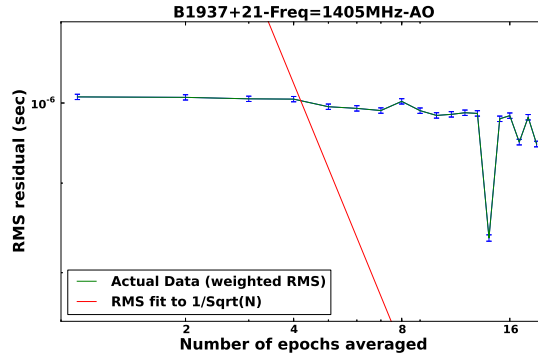


Fig. 6.—: RMS residual vs. the number of residuals averaged for PSR B1937+21 when observed at 1405MHz. The error bars on the data are too small to see. This data is from Lommen (2001) and is not a part of the NANOGrav dataset. The solid line represents the RMS fit to $N^{-1/2}$. This plot shows, as expected for this pulsar with known red noise, that the RMS residual is not proportional to $N^{-1/2}$.

4. Discussion

The main point of this paper was to determine whether RMS decreases like $N^{-1/2}$ when N , the number of adjacent observations averaged, is increased. “ N ” is to be taken as a surrogate for the dwell time per timing point, and we regard this as a test of whether increasing the dwell time per point would reduce the residual RMS or not. This is a key question in planning future NANOGrav observations.

It is important to note the limitations of the test. It represents a necessary, but not sufficient condition, of white noise in the pulsar data. In other words, all white noise will pass the root N test, but not everything that passes the root N test is white noise. For example, there may be a red noise process intrinsic to the pulsar, but the redness that such a process imprints on the timing residuals may be removed by the timing model fit. Since determining the best timing model fit was beyond the scope of this work, we assumed the current NANOGrav fitting procedure of Demorest et al. (2013). The residuals being analyzed have already passed through a timing model fit which has the property of ‘whitening’ the data, especially in the flattening of low frequency power. Thus the noise processes themselves could be red while the timing residuals pass the root N test. If a pulsar fails this test, then we can conclusively state its spectrum is not white. However, displaying an RMS proportional to root N does not necessarily mean the residuals themselves, nor the processes that created them, are true Gaussian processes.

Over-fitting is a concern for GW astronomy as it may eliminate a red noise signal from GWs by subsuming it into a fit. Indeed, this is a chief concern of Keith et al. (2013) as the expected stochastic gravitational wave background (GWB) would be a red noise signal that may have significant

power removed by an improper timing model fit, specifically in regards to fitting the time dependent nature of the DM. Some recent analyses avoid this by fitting for the timing model parameters and GW signals simultaneously (Ellis, Jenet, & McLaughlin 2012; Arzoumanian et al. 2014), while others search the post-fit residuals while accounting for the effect of the timing model fit on their signal (Jenet et al. 2006; Christy et al. 2015). It is beyond the scope of this paper to study how an individual GW source will be affected by the Demorest et al. (2013) timing model fit we assume. However, we stress that even if this test does not conclusively describe the underlying noise in a pulsar, decreasing the post-fit residual noise will increase the sensitivity to a GW signal for any post-fit analysis and thus represents an important aim of optimization studies.

We demonstrated that the residuals from 15 of the NANOGrav pulsars whose data we analyzed (B1855+09, B1953+29, J0030+0451, J0613–0200, J1012+5307, J1455–3330, J1600–3053, J1713+0747, J1744–1134, J1853+1308, J1909–3744, J1910+1256, J1918–0642, J2145–0750, and J2317+1439) are consistent with the root N trend, with a few caveats summarized here.

One striking feature of these results is that most pulsars in Figures 1,2 and 3 display a fit to root N that is better than the uncertainties would suggest, indicated by the reduced χ^2 values being smaller than 1. While it appears that most of the pulsars in NANOGrav have timing residuals that are consistent with the $N^{-1/2}$ trend, we caution the reader about this conclusion. There is some evidence that this pulsars are being overfitted by their models, however, they still follow the root N trend.

PSRs J2145–0750 and J2317+1439 do not have a lot of data. If we accumulate more data points for these pulsars, it is expected that these pulsars will continue to be consistent with the trend of the RMS being proportional to $N^{-1/2}$. On the other hand, PSR J1910+1256 has a lot of data, but since it was observed in only one frequency band, it could not be fitted for DM. The reduced χ^2 value for this pulsar is large and it is evident that DM fitting is necessary to get an accurate understanding of the data.

There were only two pulsars that showed a deviation from the root N trend, namely J1640+2224, J1643–1224. This is evident by their larger reduced χ^2 values, and by their plots showing a shallower spectrum than the $N^{-1/2}$ fit. This could be an indication of a red noise component. This is a conclusion that was reached by both Demorest et al. (2013) and Perrodin et al. (2015).

PSR B1937+21 is a known red pulsar (Figure 6), so we include it to show how a truly red pulsar will behave in our scheme. The plot shows that there is no correlation between the RMS residual and $N^{-1/2}$; this is also evident from its reduced χ^2 value. Many possible sources causing the timing noise exhibited by this pulsar have been tested, but none have been confirmed as the source of red noise (Hobbs, Lyne, & Kramer 2010; Thorsett & Phillips 1992; Shannon et al. 2013; Shannon & Cordes 2010). In any case, results from this pulsar are reassuring in that a pulsar dominated by red noise is not consistent with the root N test.

We wanted to determine whether increasing the dwell time on the NANOGrav pulsars will have the expected effect of reducing the RMS residual in each pulsar. In all cases the NANOGrav

pulsars follow the trend of $\text{RMS} \propto N^{-1/2}$ steadily, at least until observed for eight times as long ($N = 8$) in each observing session. Using this conclusion, we expect to be able to observe these 15 pulsars for up to 2-6 hours (depending on the pulsar’s current dwell time of 15-45 minutes) in one observation, before we expect to see any inconsistency with $\text{RMS} \propto N^{-1/2}$ relation. Indeed, this result has been shown for J1713+0747 in the recent, continuous 24 hour global campaign, where they observed a root T behavior Dolch et al. (2014).

Our claim that root N is a surrogate for root T assumes that the noise properties of the pulsars are stationary in time, which are discussed in §2. Recent works by Ellis, Jenet, & McLaughlin (2012) and references therein state that the NANOGrav data appears to display noise patterns that allow us to assume stationary statistics with this data set. If we can determine that the pulsar’s timing residuals display noise that is consistent with the “root T” behavior, we can be confident that increasing the dwell time will yield lower noise in the timing residuals. This is critical input for decisions regarding future observations, specifically in determining how long to spend on each pulsar.

5. Conclusions

The simplest way to decrease the noise in a PTA is to integrate over the noise for longer periods of time in each observation, e.g. go from 30-minute integrations on each pulsar to 1-hour integrations on each pulsar. However, this only works if the pulsar’s timing residuals display noise that is consistent with the root N trend. We have averaged multiple (N) adjacent integrations, a substitute to actually increasing dwell time, to see whether the timing residuals display a root N behavior. Our analysis on the NANOGrav pulsars shows that 15 of 17 are in this root N regime, with some displaying this all the way to an increase in dwell time by a factor of 8.

We note though that we only examined NANOGrav data, and the results we obtained are not necessarily the results received if this test was run on EPTA or PPTA data for these pulsars. We already see that just between the two telescopes in NANOGrav we can get different results (PSR J1713+0747), which may be different due to different DM removal algorithms (Dolch et al. 2014). Improvements in our understanding will come from attention to the dispersion removal algorithms. We saw evidence that sometimes the current algorithm over-corrects the data. Further work will consider longer data sets where red noise may be more prominent. There are many other ways to characterize the timing noise in pulsars (Perrodin et al. 2015; Ellis 2013; Cordes et al. 2015), but this test is a good first test in determining the improvability of the timing noise of a pulsar and which pulsars should be included in a PTA.

Characterizing the timing noise in this way is only one aspect of optimizing PTAs. Optimization must be done with respect to a particular goal; so is the goal of the PTAs to detect a stochastic background first (Lee et al. 2012), or a single source first (Christy et al. 2014), or is it to fully characterize the GW sources we detect? How we delegate telescope time will depend

upon the goal we choose in addition to the noise parameters. For example, if the background is in fact stochastic, we may choose different goals than if the background is dominated by a few bright sources (Babak & Sesana 2012; Sesana, Vecchio, & Colacino 2008). Knowing which pulsars’ RMS can be improved is an important first step in optimizing a PTA. In general, a lower RMS will produce more sensitive searches. The analysis done in this paper offers a measurement on the extent that the dwell time can be used to accomplish the goal of lowering the RMS.

We would like to thank Ben Stappers and Gemma Janssen for some very helpful discussions and the hospitality of Jodrell Bank Centre for Astrophysics while A.N.L. was on sabbatical. This project has been supported by NSF AST CAREER 07-48580 and NSF PIRE 0968296.

REFERENCES

- Arzoumanian, Z., Brazier, A., Burke-Spolaor, S., Chamberlin, S. J., Chatterjee, S., Cordes, J. M., Demorest, P. B., Deng, X., Dolch, T., Ellis, J. A., Ferdman, R. D., Garver-Daniels, N., Jenet, F., Jones, G., Kaspi, V. M., Koop, M., Lam, M. T., Lazio, T. J. W., Lommen, A. N., Lorimer, D. R., Luo, J., Lynch, R. S., Madison, D. R., McLaughlin, M. A., McWilliams, S. T., Nice, D. J., Palliyaguru, N., Pennucci, T. T., Ransom, S. M., Sesana, A., Siemens, X., Stairs, I. H., Stinebring, D. R., Stovall, K., Swiggum, J., Vallisneri, M., van Haasteren, R., Wang, Y., Zhu, W. W., & NANOGrav Collaboration 2014, *ApJ*, 794, 141
- Babak, S., & Sesana, A. 2012, *Phys. Rev. D*, 85, 044034
- Christy, B., Anella, R., Lommen, A., Finn, L. S., Camuccio, R., & Handzo, E. 2014, *ApJ*, 794, 163
- Christy, B., Mahany, N., Lommen, A. N., & Wymer, K. 2015, in prep
- Cordes, J. M., & Greenstein, G. 1981, *ApJ*, 245, 1060
- Cordes, J. M., Chatterjee, S., Dolch, T., Ellis, J., Finn, S., Jenet, R., Lam, M., Madison, D., McLaughlin, M., Perrodin, D., Rankin, J., Seimens, X., Vallisneri, M., & Wang, Y. 2015, in preparation
- Demorest, P. B., Ferdman, R. D., Gonzalez, M. E., Nice, D., Ransom, S., Stairs, I. H., Arzoumanian, Z., Brazier, A., Burke-Spolaor, S., Chamberlin, S. J., Cordes, J. M., Ellis, J., Finn, L. S., Freire, P., Giampanis, S., Jenet, F., Kaspi, V. M., Lazio, J., Lommen, A. N., McLaughlin, M., Palliyaguru, N., Perrodin, D., Shannon, R. M., Siemens, X., Stinebring, D., Swiggum, J., & Zhu, W. W. 2013, *ApJ*, 762, 94
- Dolch, T., Lam, M. T., Cordes, J., Chatterjee, S., Bassa, C., Bhattacharyya, B., Champion, D. J., Cognard, I., Crowter, K., Demorest, P. B., Hessels, J. W. T., Janssen, G., Jenet, F. A., Jones, G., Jordan, C., Karuppusamy, R., Keith, M., Kondratiev, V., Kramer, M., Lazarus,

- P., Lazio, T. J. W., Lee, K. J., McLaughlin, M. A., Roy, J., Shannon, R. M., Stairs, I., Stovall, K., Verbiest, J. P. W., Madison, D. R., Palliyaguru, N., Perrodin, D., Ransom, S., Stappers, B., Zhu, W. W., Dai, S., Desvignes, G., Guillemot, L., Liu, K., Lyne, A., Perera, B. B. P., Petroff, E., Rankin, J. M., & Smits, R. 2014, *ApJ*, 794, 21
- Ellis, J. A. 2013, *Classical and Quantum Gravity*, 30, 224004
- Ellis, J. A., Jenet, F. A., & McLaughlin, M. A. 2012, *ApJ*, 753, 96
- Ferdman, R. D., van Haasteren, R., Bassa, C. G., Burgay, M., Cognard, I., Corongiu, A., D’Amico, N., Desvignes, G., Hessels, J. W. T., Janssen, G. H., Jessner, A., Jordan, C., Karuppusamy, R., Keane, E. F., Kramer, M., Lazaridis, K., Levin, Y., Lyne, A. G., Pilia, M., Possenti, A., Purver, M., Stappers, B., Sanidas, S., Smits, R., & Theureau, G. 2010, *Classical and Quantum Gravity*, 27, 084014
- Gonzalez, M. E., Stairs, I. H., Ferdman, R. D., Freire, P. C. C., Nice, D. J., Demorest, P. B., Ransom, S. M., Kramer, M., Camilo, F., Hobbs, G., Manchester, R. N., & Lyne, A. G. 2011, *ApJ*, 743, 102
- Helfand, D. J., Manchester, R. N., & Taylor, J. H. 1975, *ApJ*, 198, 661
- Hellings, R. W., & Downs, G. S. 1983, *ApJ*, 265, L39
- Hemberger, D. A., & Stinebring, D. R. 2008, *The Astrophysical Journal*, 674
- Hobbs, G., Lyne, A., & Kramer, M. 2006, *Chinese Journal of Astronomy and Astrophysics Supplement*, 6, 020000–175
- Hobbs, G., Lyne, A. G., & Kramer, M. 2010, *MNRAS*, 402, 1027
- Hobbs, G., Archibald, A., Arzoumanian, Z., Backer, D., Bailes, M., Bhat, N. D. R., Burgay, M., Burke-Spolaor, S., Champion, D., Cognard, I., Coles, W., Cordes, J., Demorest, P., Desvignes, G., Ferdman, R. D., Finn, L., Freire, P., Gonzalez, M., Hessels, J., Hotan, A., Janssen, G., Jenet, F., Jessner, A., Jordan, C., Kaspi, V., Kramer, M., Kondratiev, V., Lazio, J., Lazaridis, K., Lee, K. J., Levin, Y., Lommen, A., Lorimer, D., Lynch, R., Lyne, A., Manchester, R., McLaughlin, M., Nice, D., Osłowski, S., Pilia, M., Possenti, A., Purver, M., Ransom, S., Reynolds, J., Sanidas, S., Sarkissian, J., Sesana, A., Shannon, R., Siemens, X., Stairs, I., Stappers, B., Stinebring, D., Theureau, G., van Haasteren, R., van Straten, W., Verbiest, J. P. W., Yardley, D. R. B., & You, X. P. 2010, *Classical and Quantum Gravity*, 27, 084013
- Jenet, F., Finn, L. S., Lazio, J., Lommen, A., McLaughlin, M., Stairs, I., Stinebring, D., Verbiest, J., Archibald, A., Arzoumanian, Z., Backer, D., Cordes, J., Demorest, P., Ferdman, R., Freire, P., Gonzalez, M., Kaspi, V., Kondratiev, V., Lorimer, D., Lynch, R., Nice, D., Ransom, S., Shannon, R., & Siemens, X. 2009, *ArXiv e-prints*

- Jenet, F. A., Hobbs, G. B., Lee, K. J., & Manchester, R. N. 2005, *ApJ*, 625, L123
- Jenet, F. A., Hobbs, G. B., van Straten, W., Manchester, R. N., Bailes, M., Verbiest, J. P. W., Edwards, R. T., Hotan, A. W., Sarkissian, J. M., & Ord, S. M. 2006, *ApJ*, 653, 1571
- Keith, M. J., Coles, W., Shannon, R. M., Hobbs, G. B., Manchester, R. N., Bailes, M., Bhat, N. D. R., Burke-Spolaor, S., Champion, D. J., Chaudhary, A., Hotan, A. W., Khoo, J., Kocz, J., Osłowski, S., Ravi, V., Reynolds, J. E., Sarkissian, J., van Straten, W., & Yardley, D. R. B. 2013, *MNRAS*, 429, 2161
- Lee, K. J., Bassa, C. G., Janssen, G. H., Karuppusamy, R., Kramer, M., Smits, R., & Stappers, B. W. 2012, *MNRAS*, 423, 2642
- Liu, K., Keane, E. F., Lee, K. J., Kramer, M., Cordes, J. M., & Purver, M. B. 2012, *MNRAS*, 420, 361
- Lommen, A. N. 2001. Precision Multi-Telescope Timing of Millisecond Pulsars: New Limits on the Gravitational Wave Background and other results from the Pulsar Timing Array. Ph.D. thesis, University of California, Berkeley, San Francisco
- Lommen, A. N., & Backer, D. C. 2001, *ApJ*, 562, 297
- Manchester, R. N., Hobbs, G., Bailes, M., Coles, W. A., van Straten, W., Keith, M. J., Shannon, R. M., Bhat, N. D. R., Brown, A., Burke-Spolaor, S. G., Champion, D. J., Chaudhary, A., Edwards, R. T., Hampson, G., Hotan, A. W., Jameson, A., Jenet, F. A., Kesteven, M. J., Khoo, J., Kocz, J., Maciesiak, K., Osłowski, S., Ravi, V., Reynolds, J. R., Sarkissian, J. M., Verbiest, J. P. W., Wen, Z. L., Wilson, W. E., Yardley, D., Yan, W. M., & You, X. P. 2013, *PASA*, 30, 17
- Perrodin, D., Jenet, F., Lommen, A., Finn, L., Demorest, P., Ferdman, R., Gonzalez, M., Nice, D., Ransom, S., & Stairs, I. 2015, *ArXiv e-prints*
- Sesana, A., Vecchio, A., & Colacino, C. N. 2008, *MNRAS*, 390, 192
- Shannon, R. M., & Cordes, J. M. 2010, *ApJ*, 725, 1607
- Shannon, R. M., Cordes, J. M., Metcalfe, T. S., Lazio, T. J. W., Cognard, I., Desvignes, G., Janssen, G. H., Jessner, A., Kramer, M., Lazaridis, K., Purver, M. B., Stappers, B. W., & Theureau, G. 2013, *ApJ*, 766, 5
- Siemens, X., Ellis, J., Jenet, F., & Romano, J. D. 2013, *ArXiv e-prints*
- Thorsett, S. E., & Phillips, J. A. 1992, *ApJ*, 387, L69
- Wackerly, D. D., Mendenhall III, W., & Scheaffer, R. L. 2008. *Mathematical Statistics with Applications*, p. 353. Brooks/Cole, Cengage Learning, seventh edition

